Learning Robust Rule Representations for Abstract Reasoning via Internal Inferences

Anonymous Author(s)
Affiliation
Address
email

Abstract

Abstract reasoning, as one of the hallmarks of human intelligence, involves collecting information, identifying abstract rules, and applying the rules to solve new problems. Although the neural networks have achieved human-level performances in several tasks, the abstract reasoning techniques still far lag behind due to the complexity of learning and applying the logic rules, especially in an unsupervised manner. In this work, we propose a novel framework, ARII, that learns rule representations for *Abstract Reasoning via Internal Inferences*. The key idea is to repeatedly apply a rule to different instances in hope of having a comprehensive understanding (i.e., representations) of the rule. Specifically, ARII consists of a rule encoder, a reasoner, and an internal referrer. Based on the representations produced by the rule encoder, the reasoner draws the conclusion while the referrer performs internal inferences to regularize rule representations to be robust and generalizable. We evaluate ARII on two benchmark datasets, including PGM and I-RAVEN. We observe that ARII achieves the new state-of-the-art records on the majority of the reasoning tasks, including most of the generalization tests in RPM. In particular, ARII beats the previous best models by 23.2% on the generalization test of held-out attribute pairs on RPM.

1 Introduction

Abstract reasoning, the ability to extract patterns and rules from concrete instances and apply them to solve new problems, is one of the hallmarks of human intelligence. It is a critical topic to endow neural networks with the capacity of abstract reasoning on the road from artificial intelligence (AI) to human-like intelligence. As "thinking in pictures" is one of the most effortless and natural ways for humans to perform inference, Raven's Progressive Matrices (RPM) test [1] is a widely accepted task to evaluate AI's reasoning ability. As shown in Fig 1, a RPM problem contains an incomplete 3×3 matrix where the bottom-right entry is missing. The subjects are aware of that the rows in the matrix implicitly share identical rules and are asked to pick the suitable answer from the choices that would best complete the missing entry. Considering that the RPM test is shown to be highly correlated with real intelligence [2] in cognitive and psychological science, AI community recently presents a huge interest in this task to explore the model's capacity of abstract reasoning [3, 4, 5, 6, 7].

In the early years, computational models for RPM usually assume the access to the symbolic representations of the images and thus solve RPM with heuristics. Recently, various neural networks are proposed to accomplish abstract reasoning with the help of the abundant reasoning data (such as PGM [5], RAVEN[7], I-RAVEN [8]). These models mainly treat the RPM problem as a classification task for multiple choice panels based on the rules hidden in rows or columns. For example, CoPINet [9] develops a contrastive perceptual inference network to improve the feature extraction capacity [7].

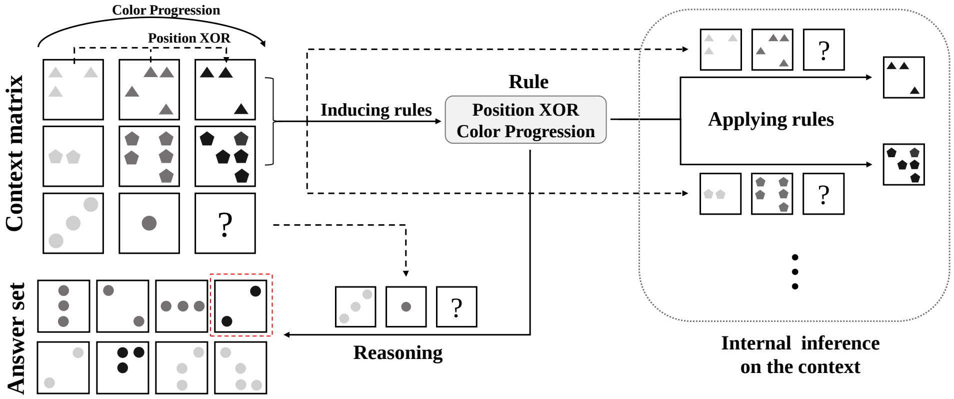

Figure 1: An example of RPM problem and the general solution of this work.

SCL designs compositions of neural networks according to the specific characteristics of the RPM problems (e.g., the number of the attributes) [10].

Although existing models have achieved impressive performance on abstract reasoning, the critical capacity, i.e. generalization to different environments remains unsolved [5, 11, 12, 13]. In particular, Małkiński [14] report that, the performances of the current models would significantly decrease even if the test images changes slightly [5, 11, 12, 13]. For example, a generalization regime (i.e., an evaluation task) in the PGM dataset is extrapolation, where the model is trained on the images with color or size restricted to the lower half of the value set and tested on images taking these values from the upper half. MLRN [13] achieves nearly perfect accuracy in the normal test of the PGM dataset, but fails completely in the extrapolation regime, yielding only slightly above chance. This reveals that these models are just overfitted to the specific data rather than mastering the reasoning essence, reflected by low generalization to distracting features [15].

This paper provides a novel framework that ameliorates the reasoning generalizability by learning a robust rule representation. To achieve it, we make two assumptions of the rule representation for abstract reasoning. On the one hand, we assume the space of the abstract rules is finite and usually not large. Thus, we propose a rule encoder that produces discrete rule representations by vector quantisation [16]. On the other hand, we assume the rule representation should be invariant to specific instances or distracting features. In human reasoning, people usually apply an abstract rule to different instances for several times to deepen the understanding of the rule. We mimic this cognitive process by introducing an internal inference process based on the learned rule representations. Specifically, we randomly mask one panel of the first two rows and ask the referrer to infer the masked panel based on the rule representation. We perform the internal inference for multiple times to make the rule representation invariant to specific instances. Based on these instance-invariant representations, we apply another neural network to make conclusions according to the specific context images. Therefore, we call our model ARII, the abbreviation of "abstract reasoning via internal inferences."

We first conduct comprehensive empirical experiments on the I-RAVEN [8] datasets. Compared with the current state-of-the-art models (e.g., SCL [10] and CoPINet [9]), experiments show that our model achieves new records on four of the seven single training tasks in the I-RAVEN datasets. As the generalization tests can better reflect the real reasoning ability of a model, we also evaluate ARII on the seven generalization regimes of the PGM dataset and observe that ARII outperforms the other competing method in the five regimes. In particular, ARII beats the previous best models by 23.2% on the generalization test of held-out attribute pairs on PGM.

To summarize, this work makes three contributions as follows:

- We propose a novel framework that learns rule representations for abstract reasoning by internal inferences. In particular, we introduce a rule encoder to produce discrete rule representations by vector quantisation. We design an internal inference process to learn an instance-invariant and robust rule representation.
- Our model achieves superior results to state-of-the-art methods on the majority of tasks (four out of seven) on I-RAVEN and better generalization performance on most PGM regimes.

- Visualization results on the rule representations indicate that the learned representations can be automatically clustered with respect to the rule categories. Deep analysis shows that we can identify some features in the discrete representations for a specific reasoning rule, validating that the representations are interpretable and instance-invariant. By virtue of these characteristics, we could further explore the composition of the abstract rules in future work.

2 Related Work

RPM problems are firstly investigated in the cognitive science community to better understand intelligence, and many computational models are proposed to address this test since 1990s. Carpenter et al. [2] develop a production system that takes hand-coded textual descriptions of problems as input and predicts the answer. In addition, Lovett et al. [17] combine spatial representations with analogical comparison via structure-mapping to solve the PRM problems. Overall, these cognitive models mainly adopt hand-craft or symbolic representations for the rules and images, and solve specific problem sets[1] with only a limited number of hand-craft instances in cognitive science [17, 19, 20].

Recently, RPM problems have gained a lot of attention in the AI field to explore abstract reasoning capability. The Procedurally Generating Matrices (PGM) dataset [5] together with the Relational and Analogical Visual rEasoNing (RAVEN) dataset [7] expands the size of RPM instances through automatic generation algorithms, serving as the benchmark datasets for deep learning network to study abstract reasoning. However, Hu et al. [8] found severe defects (a short cut for predictions) existing in the RAVEN dataset and create an unbiased version called I-RAVEN dataset to solve it. Therefore, we evaluate our method on the PGM and I-RAVEN datasets rather than RAVEN.

Based on the above datasets, various end-to-end approaches have been proposed to study the abstract reasoning ability. The typical architectures in computer vision, that simply use CNN as visual feature extractor followed by MLP [3] or LSTM [5, 21] to process the features from all the image panels, are shown to lack the reasoning ability and struggle in the RPM test. To improve the reasoning capacity, Relation Network [22] is equipped and extended in many models, including Wild Relation Network [5], Multi-scale Relation Network [23], Multi-Layer Relation Network [13].

Although the above models obtain elegant performance on the RAVEN and I-RAVEN datasets, they still fail to achieve satisfactory generalization results on the PGM dataset, reflecting the overfitting issue of these reasoning models. Auxiliary training with additional labels [24, 11, 15] is therefore utilized to develop representations that are more amenable to generalization by informing the meta-targets which encode relevant relations and attributes. However, it requires additional prior information, which is not a general way to address the reasoning problem.

3 Methodology

3.1 Problem formulation

Raven's Progressive Matrices (RPM) is a well-known IQ test [1, 18] to measure the reasoning ability of humans. The RPM test is conducted on a 3×3 matrix where the rows or columns comply with an identical rule. Subjects are presented with an incomplete matrix where an entry on the third row is missing, and are asked to select a candidate answer from the choice set to complete the matrix.

Formally speaking, a RPM problem contains 16 image panels $X = \{x_i\}_{i=1}^{16}$ divided into 8 context images $X_c = \{x_i\}_{i=1}^{8}$ and 8 candidate answer images $X_a = \{x_i\}_{i=9}^{16}$. The 8 context images are placed in a 3×3 matrix with the last element blank. For each particular data point, the three rows in the matrix implicitly share the identical abstract rule. Given the X, the machine is asked to select a candidate answer image from X_a to best complete the matrix (i.e. adhering to the underlying abstract rule in context images). The correct answer is denoted by x^*, where $x^* \in X_a$.

3.2 The ARII model

We introduce a novel framework with internal inferences to solve RPM problems. In particular, our model consists of three modules: the rule encoder, the reasoner, and the internal inferrer. The

[1] Standard Progressive Matrices [18] contains 60 problems

rule encoder induces the rule representation from the context matrix. The inferrer performs internal inferences to regularize the rule representations to be robust and instance invariant. The reasoner draws the reasoning conclusion based on the rule representations. The rest of this section elaborates on these components and the training process.

3.3 Rule encoder

To tackle this reasoning problem, an ideal reasoning process is to figure out the underlying rule based on the given context images. To achieve this, we aim to learn the rule representations $\boldsymbol{r}$ using an effective encoder. In principle, the rule can be extracted from particular row of images. But the above extraction has the potential to make mistakes since a single row of images may satisfy multiple rules. Therefore, to guarantee the adequate information for rule extraction, we propose to encode the first two rows of images to represent the underlying rule, given by

$$\boldsymbol{r}_{1\&2} = \text{RuleEnc}(\{x_i\}_{i=1}^{6}), \tag{1}$$

where $\boldsymbol{r}_{1\&2}$ stands for the representation of the rule underlying the first two rows in the given matrix. x_i is the i-th image panel in a PRM problem and the first to the sixth image panels constitute the first two rows of the matrix. Rule-Enc stands for the rule encoder in the ARII model. In the rest of this section, we first obtain the image encodings and then build the rule representations based on the the encodings of the involved images.

Image encodings. As each row contains three separated images, we adopt convolutional neural network (CNN) blocks to get the feature map ($\boldsymbol{f}$) for each image separately.

$$\boldsymbol{f}_i = \text{CNN}(x_i), \quad i = 1, 2 \ldots, 6. \tag{2}$$

Once we get the feature map, we further fuse the features of different positions in the feature map. Intuitively, the rule of RPM is highly correlated with visuospatial ability [25] and usually lies in the same position of different panels. Therefore, we first divide the feature map into multiple groups; each group can be considered to contain information from a certain position. Then we apply a fully connected layer (FC) to each group to further extract group features, and concatenate the group features into output features, computed by

$$\boldsymbol{z}_i = \text{ImageEnc}(x_i) = ||_k^{K_z}[\text{FC}(\boldsymbol{f}_i^k)], \quad i = 1, 2 \ldots, 6, \tag{3}$$

where $||$ stands for the concatenation operation of the vectors. $\boldsymbol{f}_i^k$ is k-th group features after splitting original $\boldsymbol{f}_i$ into K_z groups. Similar to the scattering transformation in SCL [10], the group features $\{\boldsymbol{f}_i^k\}$ are divided evenly from the feature map $\boldsymbol{f}_i$. Finally, the K_z new groups of the features are concatenated (denoted by $||_k^{K_z}$) to obtain the i-th image encodings z_i.

Continuous rule representations. Next, the rule encoder fuses the image encodings and extracts the rule representations. Similar to the processing of images, we extract the relation corresponding to the different positions of the six image encodings as Fig 2. Specifically, the encodings of six images are first divided into K_r groups independently. The groups at the same location in six image encodings are combined together and fed into a fully connected layer to further extract the relation feature. Finally, the multiple relation features are merged to form rule features as follows:

$$\boldsymbol{r}_c = ||_k^{K_r}[\text{FC}(||_{i=1}^{6} z_i^k)], \tag{4}$$

where $\boldsymbol{z}_i^k$ is the k-th group of the i-th image encodings $\boldsymbol{z}_i$. $||_{i=1}^{6} z_i^k$ means six k-th group features from embeddings are concatenated, and fed into a fully connected layer (FC) to get the k-th relation features. We further merge the K_r relation features and obtain the continuous rule representations $\boldsymbol{r}_c$.

Discrete rule representations. Note that the above rule representations $\boldsymbol{r}_c$ are continuous variables, and are dependent on the specific instances. In this work, we suppose that the underlying rules should be independent of the specific instances and can be reused in different problems which share the same rules. Based on this assumption, the discrete and finite representations are more suitable to describe abstract rules.

Therefore, we propose to discretize the latent representations of the rules via vector quantisation (VQ) [16]. In particular, the rule encoder maintains a discrete codebook $E \in \mathbb{R}^{K_e \times D}$. K_e is the number of the discrete code, and D is the dimensionality of each discrete code E_k. We measure the L2 distance between the continuous representation $\boldsymbol{r}_c$ and code vectors in the codebook. For each vector $\boldsymbol{r}_c^l$ in $\boldsymbol{r}_c \in \mathbb{R}^{K_r \times D}$, where K_r is the number of the continuous vector and D is the dimensionality of each continuous vector $\boldsymbol{r}_c^l$, the code vector that yields the minimum distance is taken to obtain the discrete

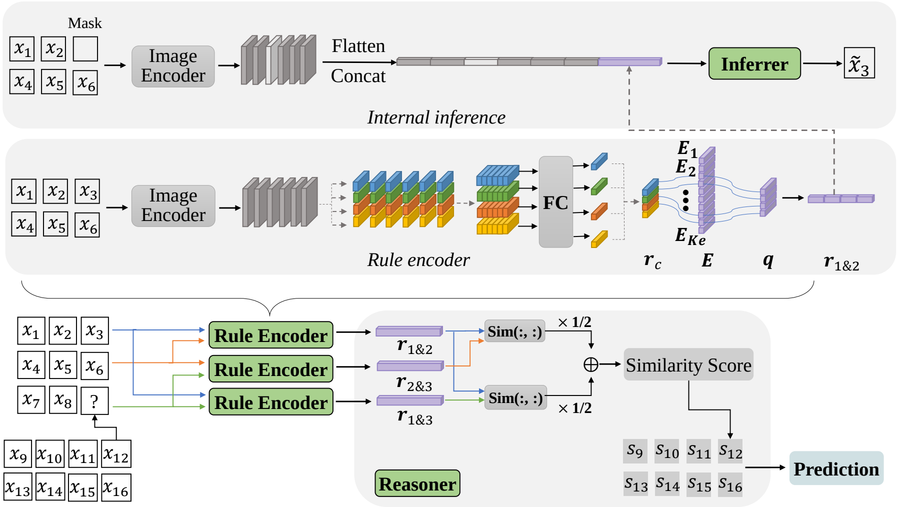

Figure 2: The architecture of ARII.

rule representation $\boldsymbol{q}_l$. The detailed computations are

$$\boldsymbol{q}_l = E_k, \quad \text{where} \quad k = \underset{j\in\{1,\dots,K_e\}}{\arg\min} \; \|\boldsymbol{r}_c^l - E_j\|_2, \tag{5}$$

where $\boldsymbol{q}_l$ is the closest quantized vector for the continuous vector $\boldsymbol{r}_c^l$. Via vector quantisation, we can find the closest code for the given continuous rule representations, i.e.,

$$\boldsymbol{r}_{1\&2} = \text{RuleEnc}(\{x_i\}_1^6) = ||_{l=1}^{K_r}[\boldsymbol{q}_l]. \tag{6}$$

To make the above vector quantisation work, we need to train both the neural networks and the codebook in the rule encoder towards the minimum of the distance between the continuous and discrete representations. The objective function of vector quantisation for a particular data point is

$$\mathcal{J}^{\text{vq}}(X_c) = ||\boldsymbol{r}_c - \text{tru}(\boldsymbol{r}_{1\&2})||_2^2 + ||\text{tru}(\boldsymbol{r}_c) - \boldsymbol{r}_{1\&2}||_2^2, \tag{7}$$

where $\text{tru}(\cdot)$ performs the gradient truncation during forward computation. In this way, we can derive the discrete rule representations, which is expected to be interpretable and instance-invariant.

3.4 Reasoner

The reasoner is to draw conclusions (i.e., the selection of answer images) based on the extracted rule and the specific context (i.e., the images on the third row). That is, the reasoner applies the extracted rule to the third row and figure out which candidate answer could best complete the missing entry.

According to this standard, we therefore extract the rule that the third row implicates. Since we have 8 candidate answer images (i.e., X_a), there are 8 rules for the third row with the different answer images in the missing entry. However, the rule encoder is designed to take two rows of images as inputs and yield the rule representations. Therefore, we combine the third row with the first row to derive the rule that these two rows implicitly share, computed by

$$\boldsymbol{r}_{1\&3}^j = \text{RuleEnc}(\{x_i | i = 1, 2, 3, 7, 8, j\}), \quad j = 9, \dots, 16 \tag{8}$$

where $\boldsymbol{r}_{1\&3}^j$ denotes the rule representations of the rule underlying the first and the third row when the third row is completed with the j-th answer image. Similarly, we can obtain the rule representations of the rule underlying the second and third row, given by

$$\boldsymbol{r}_{2\&3}^j = \text{RuleEnc}(\{x_i | i = 4, 5, 6, 7, 8, j\}), \quad j = 9, \dots, 16 \tag{9}$$

Based on the derived rule representations for the third row, the reasoner next measures the similarity between these rule representations and the reference rule (i.e., $\boldsymbol{r}_{1\&2}$) and selects the most similar one as the prediction. In particular, the reasoner measures the similarity of two rules by calculating the inner product of the corresponding representations. For example, the similarity between the rule $\boldsymbol{r}_{1\&3}$ and the reference rule is calculated by

$$\text{sim}(\boldsymbol{r}_{1\&3}^j, \boldsymbol{r}_{1\&2}) = \frac{e^{\boldsymbol{r}_{1\&3}^j \cdot \boldsymbol{r}_{1\&2}}}{\sum_{i=9}^{16} e^{\boldsymbol{r}_{1\&3}^j \cdot \boldsymbol{r}_{1\&2}}}, \quad j = 9, \dots, 16, \tag{10}$$

where sim$(\cdot)$ is the similarity function of two rule representations. Similarly, the reasoner derives the similarity between the rule $\boldsymbol{r}_{2\&3}$ and the reference rule by

$$\text{sim}(\boldsymbol{r}^j_{2\&3}, \boldsymbol{r}_{1\&2}) = \frac{e^{\boldsymbol{r}^j_{2\&3} \cdot \boldsymbol{r}_{1\&2}}}{\sum_{i=9}^{16} e^{\boldsymbol{r}^j_{2\&3} \cdot \boldsymbol{r}_{1\&2}}}, \quad j = 9, \ldots, 16. \tag{11}$$

Based on the similarities between individual rules, the reasoner then predicts the candidate answer y.

$$y = \max_{j \in \{9,\ldots,16\}} \frac{1}{2}[\text{sim}(\boldsymbol{r}^j_{1\&3}, \boldsymbol{r}_{1\&2}) + \text{sim}(\boldsymbol{r}^j_{2\&3}, \boldsymbol{r}_{1\&2})]. \tag{12}$$

For the optimization of the reasoner, we adopt the cross entropy loss to guide the reasoner make select the correct answer images, given by

$$\mathcal{J}^{\text{re}}(X) = -\frac{1}{2}[\log \text{sim}(\boldsymbol{r}^*_{1\&3}, \boldsymbol{r}_{1\&2}) + \log \text{sim}(\boldsymbol{r}^*_{2\&3}, \boldsymbol{r}_{1\&2})] \tag{13}$$

3.5 Internal inferences

Human usually apply an abstract rule to different instances for several times to deepen the understanding of the rule. We mimic this cognitive process by performing internal inferences based on the rule representations. In the internal inference, we introduce another reasoner to address the reasoning task on the two rows of images when the rule representations are available. In this way, our method ARII could also better “understand” the rule and have more robust rule representations.

In particular, the first and second rows are used in internal inference process. We first extract the rule representations $\boldsymbol{r}_{1\&2}$ of these rows and then randomly mask one of the six images $\{x_i\}_{i=1}^6$ by a white blank image. We coin the blank image as $\hat{x}_m$, where m is the index of the masked images. Thus, the masked two rows can be expressed by

$$I_m = \{x_i | i \in \{1, 2, 3, 4, 5, 6\} \backslash m\} \cup \{\hat{x}_m\} \tag{14}$$

where $\{1, 2, 3, 4, 5, 6\} \backslash m$ stands for a set excluding the index m and we insert blank image $\hat{x}_m$ in the original m-th position. Next, we introduce another neural network named inferrer that takes the rule representations and the encodings of the images in the masked two rows as inputs, and predicts the masked image.

$$\tilde{x}_m = \text{Inferrer}(\text{ImageEnc}(I_m), \boldsymbol{r}_{1\&2}), \tag{15}$$

where Inferrer is another CNN model. $\tilde{x}_m$ stands for the predicted image for the incomplete rows, and ImageEnc(I_m) derives the encoding of I_m by Equation 2 and 3. To avoid using additional data in our internal inference, we formulate the above prediction as to the generation process. That is to say, the inferrer aims to generate the masked image x_m at the pixel level.

In addition, we repeat the above internal inferences for 6 times by masking each image to learn more robust rule representations. We adopt mean squared error (MSE) as the objective function to optimize the inferrer as well as the rule encoder. In this way, we obtain the overall objective function $\mathcal{J}^{\text{if}}$ by collecting the predictions of these internal inference processes, given by

$$\mathcal{J}^{\text{if}}(X_c) = \frac{1}{6} \sum_{m=1}^{6} ||x_m - \tilde{x}_m)||_2^2 \tag{16}$$

3.6 Optimization of ARII

As introduced in the section on problem formulation, the major goal of our method ARII is to select a candidate answer image for the incomplete matrix as accurately as possible (as shown in Equation 13). In the meanwhile, we assume the rule representations are discrete and can be reused in internal inferences. That is, apart from the major goal, we have two additional objectives, i.e., the objective of the vector quantisation process and the objective of the internal inferences. Therefore, we combine these three objectives together for the optimization of the individual components of ARII, given by

$$\mathcal{J} = \sum_{X \in \mathcal{D}} \lambda_{\text{re}} \mathcal{J}^{\text{re}}(X) + \lambda_{\text{vq}} \mathcal{J}^{\text{vq}}(X_c) + \lambda_{\text{if}} \mathcal{J}^{\text{if}}(X_c), \tag{17}$$

where the context images X_c is parts of the given data point X and $\mathcal{D}$ is the dataset. λ_{re}, λ_{vq} and λ_{if} are the three hyper-parameters that coordinates the importance of the components in ARII.

Table 1: Test accuracy of individual models on I-RAVEN.

	Test Accuracy (%)							
Model	Average	Center	2×2 Grid	3×3 Grid	L-R	U-D	O-IC	O-IG
LSTM [7]	12.5	12.3	13.3	12.8	12.7	10.3	12.9	13.1
WReN [5]	17.8	23.3	18.1	17.4	16.5	15.2	16.8	17.3
CNN+MLP [5]	12.9	12.9	13.2	12.7	11.5	13.5	12.9	13.7
Resnet-18 [7]	14.5	20.8	12.9	14.3	13.2	13.4	13.8	12.9
LEN [15]	28.4	42.5	21.1	19.9	27.6	28.1	32.9	27.0
CoPINet [9]	38.6	50.4	30.9	28.5	40.0	40.8	42.7	36.9
SCL [10]	85.4	**99.8**	72.4	64.2	**99.5**	**99.4**	98.6	64.2
Ours	**91.1**	98.9	**88.2**	**78.9**	97.8	90.3	**98.7**	**85.1**

4 Experiment

4.1 Datasets

PGM. Each matrix in PGM is governed by abstract rules, which are sampled from a rule set $\mathcal{R} = \{[s, o, a] : s \in \mathcal{S}, o \in \mathcal{O}, a \in \mathcal{A}\}$, where $\mathcal{S}$, $\mathcal{O}$, $\mathcal{A}$ are primitive sets of relations, objects and attributes, respectively. $\mathcal{S} = \{\text{progression, XOR, OR, AND, consistent union}\}$, $\mathcal{O} = \{\text{shape, line}\}$, $\mathcal{A} = \{\text{size, type, color, position, number}\}$. There are eight regimes in PGM. The easiest one is called neutral where the training and test set are sampled from the same distribution, and the others are generalization regimes where the training and test data differ in the pre-defined ways. The generalization regimes consists of seven variants: interpolation, extrapolation, held-out triples (H.O.Triples), held-out attribute pairs (H.O.A.P.), held-out pairs of triples (H.O.T.P.), held-out shape-colour (H.O.S-C) and held-out line-type (H.O.L-T). More details can be found in Barrett et al. [5].

RAVEN and I-RAVEN. The RAVEN and I-RAVEN datasets are extensions to PGM. They share an identical set of attributes but differ in the following attributes: progression, constant, union and arithmetic. I-RAVEN is adapted from RAVEN dataset for its biased answer sets which may lead to a shortcut solution that only candidate answers can yield accurate answers [8].

4.2 Competing methods

We compare our model with several state-of-the-art models, including CNN + LSTM [5], ResNet-based [26] image classifier, Wild ResNet [5], Wild Relation Network (WReN) [5], Contrastive Perceptual Inference network (CoPINet) [9], Logic Embedding Network (LEN) [15], Scattering Compositional Learner (SCL) [10], Stratified Rule-Aware Network (SRAN) [8], Multi-scale Relation Network (MRNet) [23], and Multi-Layer Relation Network (MLRN) [13]. Note that our model is trained end to end and needs solely the ground truth answer label without auxiliary information. We report the result of the baseline models without auxiliary loss for fair comparison.

4.3 Experiment setup

In ARII, the convolutional block used in rule encoder is 4-layer CNN with kernel size 3 and channels of $\{16, 16, 32, 32\}$. The group number K_z for extracting image encodings is 10. The number of codes K_r in the rule representation is set to 80. The dimensions of the codebook E are $K_e = 512$ and $D = 5$. The inferrer is another CNN block (3-layer CNN with kernel size 3 and channels $\{64, 32, 1\}$) with upsampling techniques. During training, the weights in the objective function $\{\lambda_{\text{re}}, \lambda_{\text{vq}}, \lambda_{\text{if}}\}$ are sampled from either $\{1, 1, 1\}$ or $\{0.1, 0.1, 0.8\}$.

In our experiments, we first evaluate the models' reasoning ability I-RAVEN since it is easier than PGM. Then we the measure generalization capacity of reasoning on each regimes of PGM. For model training, we use single training setting [10], where the model is trained and tested on each configuration or regime separately. Since the rules in PGM exist in either rows or columns, we transpose the context matrix of all problems in PGM and add them for training and testing to fit our row-wise setting of rule encoder.

4.4 Results

Table 1 shows the test performance of individual models on I-RAVEN dataset. We observe that the typical architectures in computer vision, that simply uses CNN as visual feature extractor followed

Table 2: Test accuracy of different models on PGM

	Test Accuracy (%)							
Model	Neutral	Interpolation	H.O.A.P.	H.O.T.P.	H.O.Triples	H.O.L-T	H.O.S-C	Extrapolation
CNN MLP [5]	33.0	-	-	-	-	-	-	-
CNN LSTM [5]	35.8	-	-	-	-	-	-	-
ResNet-50 [5]	42.0	-	-	-	-	-	-	-
Wild-ResNet [5]	48.0	-	-	-	-	-	-	-
CoPINet [9]	56.4	-	-	-	-	-	-	-
WReN $\beta = 0$ [5]	62.6	64.4	27.2	41.9	19.0	14.4	12.5	17.2
VAE-WReN [27]	64.2	-	36.8	43.6	24.6	-	-	-
MXGNet $\beta = 0$ [11]	66.7	65.4	33.6	43.3	19.9	16.7	16.6	18.9
LEN $\beta = 0$ [15]	68.1	-	-	-	-	-	-	-
DCNet [12]	68.6	59.7	-	-	-	-	-	17.8
T-LEN $\beta = 0$ [15]	70.3	-	-	-	-	-	-	-
SRAN [8]	71.3	-	-	-	-	-	-	-
Rel-Base [28]	85.5	-	-	-	-	-	-	22.1
SCL [10]	88.9	-	-	-	-	-	-	-
MRNet [23]	93.4	68.1	38.4	55.3	25.9	**30.1**	**16.9**	19.2
MLRN [13]	**98.0**	57.8	-	-	-	-	-	14.9
Ours	88.0	**71.6**	**61.6**	**58.6**	**30.5**	20.1	15.4	**31.6**

Table 3: Ablation study on two regimes in PGM

Regime	w/o discretization	w/o internal inference	w/o both	ARII
Interpolation	60.3	42.4	38.5	**71.6**
H.O.A.P	42.7	32.2	32.6	**61.6**

by MLP or LSTM, fail to yield satisfactory reasoning results. More advanced models for abstract reasoning such as LEN and SCL significantly improve the performance. In particular, the previously state-of-the-art model SCL achieves nearly 100% accuracy on the configurations of Center, L-R, U-D, and O-IC, but SCL could not make similar success on the other configurations. We conjecture that the reasoning complexity of these four configurations are relative low and easy. As for our method, ARII performs similarly to SCL on the above four configurations but largely outperforms it on the other three more difficult configurations, leading to a notably higher average score on I-RAVEN.

In addition, Table 2 presents the performance on the PGM dataset. For the neutral regime, our model achieves decent result that is better than majority of baseline models, although it does not outperform state-of-the-art models such as MRNet and MLRN. Note that MLRN achieves near perfect accuracy in the neutral regime due to the sophisticated design which could not applied to other problems. For example MLRN draw on magnitude encoding to describe the intensities of the grayscale images. More importantly, neutral regime is not our main focus of metric, since it could hardly indicate the reasoning ability and generalization towards real intelligence.

PGM also allows us to investigate the generalization capacity of the models under various regimes. We observe from Table 2 that although MLRN achieves superior performance on neutral, it is prone to overfitting and performs poorly on the interpolation and extrapolation regimes, clearly indicating MLRN is overfitted to the neutral setting. On the contrary, the proposed internal inference in ARII severs as the regularities of the rule representations, making the rule representations robust and instance-invariant. As a result, our model outperforms all other methods on five of the seven generalization regimes (except for Held-out shape-colour and Held-out line-type) in PGM dataset. In particular, the accuracy of ARII increases by a sizable margin over the baselines in the Held-out Attribute Pairs and Extrapolation regimes (above 20% and nearly 10% respectively), further validating the superior general ability of abstract reasoning.

4.5 Ablation study

We analyze ARII in more detail to validate the effectiveness of the proposed components on two regimes in the PGM dataset (Table 3). In the interpolation regime, we first evaluate the effectiveness of discrete representation. The result of ARII without discretization decreases largely by around 10%, which shows the discrete representation plays its role in generalization of abstract reasoning. The performance is also largely declined by around 30% when the internal inference is removed, suggesting that the internal inference is indeed vital to learn a more robust rule representation for abstract reasoning. Similar results can be found in H.O.A.P. regime.

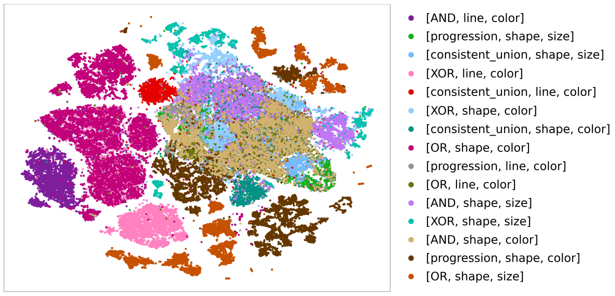

Figure 3: Visualization of rule embeddings extracted rule encoder.

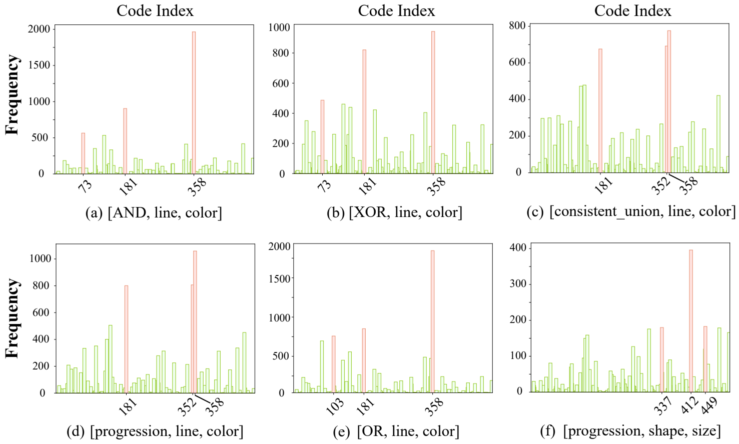

(a) [AND, line, color]
(b) [XOR, line, color]
(c) [consistent_union, line, color]
(d) [progression, line, color]
(e) [OR, line, color]
(f) [progression, shape, size]

Figure 4: The selected frequency of code in the representations of the rules.

4.6 Visualization of rule representations

Then, we try to validate whether ARII has learned the instance-invariant representations. We first obtain all the rule representations in the test set of the interpolation regime of PGM, and use the representations derived from the problems which contain only a single rule (i.e., a triple $\{[s, o, a]\}$). The rule representations are projected to 2D space by t-distributed stochastic neighbor embedding (t-SNE) [29] in Fig 3. We observe that the rule representations are clustered according to individual rule triples. Note that these clusters for each rule are formed without supervision of the rule labels. And the representations are extracted from the generalization test set and has a different distribution from the training set. The clustered representations show that these rule representations are universal and independent to the specific instances, even to the out-of-distribution brand new instances.

Taking one step further, we investigate whether the discrete rule representation is interpretable. In particular, we want to see the composition of the representations for each specific rule. Here, we take the rules related to the line object and the color attribute (totally five rules, i.e., [$s \in \mathcal{S}$, line, color], denoted by the [·,line, color] rules) as an example. We first collect the rule representations from all the instances governed by these rules, which are sampled from the codebook E. Then we calculate the selected frequencies of the codes and visualize their distributions. Figure 4 (a-e) shows that all the five rules share the same codes E_{358} and E_{181} in their top-3 codes, indicating that the codes E_{358} and E_{181} are very relevant to the [·,line, color] rules. In addition, these codes are also specific to these rules, since they rarely appear in the dissimilar rules such as the rule [progression, shape, size] (Fig 4 (f)). These results reveal that the rule representations learned by ARII are moderately interpretable.

5 Conclusion

In this work, we propose a novel architecture ARII that learns robust rule representations for abstract reasoning via internal inferences. Experiments on benchmark datasets (I-RAVEN and PGM) show that ARII outperforms previous state-of-the-art methods without using auxiliary annotations on the majority of the reasoning tasks. Moreover, the rule representations of ARII present meaningful and interpretable characteristics, facilitating the exploration of the composition of the rules in future work.

References

[1] John C Raven and JH Court. *Raven's progressive matrices*. Western Psychological Services Los Angeles, CA, 1938.

[2] Patricia A Carpenter, Marcel A Just, and Peter Shell. What one intelligence test measures: a theoretical account of the processing in the raven progressive matrices test. *Psychological review*, 97(3):404, 1990.

[3] Dokhyam Hoshen and Michael Werman. Iq of neural networks. *arXiv preprint arXiv:1710.01692*, 2017.

[4] Ke Wang and Zhendong Su. Automatic generation of raven's progressive matrices. In *IJCAI*, 2015.

[5] David Barrett, Felix Hill, Adam Santoro, Ari Morcos, and Timothy Lillicrap. Measuring abstract reasoning in neural networks. In *ICML*, pages 511–520, 2018.

[6] Jacek Mańdziuk and Adam Żychowski. Deepiq: A human-inspired ai system for solving iq test problems. In *IJCNN*, pages 1–8, 2019.

[7] Chi Zhang, Feng Gao, Baoxiong Jia, Yixin Zhu, and Song-Chun Zhu. Raven: A dataset for relational and analogical visual reasoning. In *CVPR*, pages 5317–5327, 2019.

[8] Sheng Hu, Yuqing Ma, Xianglong Liu, Yanlu Wei, and Shihao Bai. Stratified rule-aware network for abstract visual reasoning. In *AAAI*, pages 1567–1574, 2021.

[9] Chi Zhang, Baoxiong Jia, Feng Gao, Yixin Zhu, Hongjing Lu, and Song-Chun Zhu. Learning perceptual inference by contrasting. *NeurIPS*, 32, 2019.

[10] Yuhuai Wu, Honghua Dong, Roger Grosse, and Jimmy Ba. The scattering compositional learner: Discovering objects, attributes, relationships in analogical reasoning. *arXiv preprint arXiv:2007.04212*, 2020.

[11] Duo Wang, Mateja Jamnik, and Pietro Lio. Abstract diagrammatic reasoning with multiplex graph networks. In *ICLR*, 2020.

[12] Tao Zhuo and Mohan Kankanhalli. Effective abstract reasoning with dual-contrast network. In *ICL*, 2021.

[13] Marius Jahrens and Thomas Martinetz. Solving raven's progressive matrices with multi-layer relation networks. In *IJCNN*, pages 1–6, 2020.

[14] Mikołaj Małkiński and Jacek Mańdziuk. Deep learning methods for abstract visual reasoning: A survey on raven's progressive matrices. *arXiv preprint arXiv:2201.12382*, 2022.

[15] Kecheng Zheng, Zheng-Jun Zha, and Wei Wei. Abstract reasoning with distracting features. *NeurIPS*, 32, 2019.

[16] Aaron Van Den Oord, Oriol Vinyals, et al. Neural discrete representation learning. *NeurIPS*, 30, 2017.

[17] Andrew Lovett, Kenneth Forbus, and Jeffrey Usher. A structure-mapping model of raven's progressive matrices. In *Proceedings of the Annual Meeting of the Cognitive Science Society*, volume 32, 2010.

[18] John C Raven, John Hugh Court, and John Earle Raven. *Standard progressive matrices*. Australian Council for Educational Research Limited, 1989.

[19] Maithilee Kunda, Keith McGreggor, and Ashok K Goel. A computational model for solving problems from the raven's progressive matrices intelligence test using iconic visual representations. *Cognitive Systems Research*, 22:47–66, 2013.

[20] Claes Strannegård, Simone Cirillo, and Victor Ström. An anthropomorphic method for progressive matrix problems. *Cognitive Systems Research*, 22:35–46, 2013.

[21] Sepp Hochreiter and Jürgen Schmidhuber. Long short-term memory. *Neural computation*, 9(8):1735–1780, 1997.

[22] Adam Santoro, David Raposo, David G Barrett, Mateusz Malinowski, Razvan Pascanu, Peter Battaglia, and Timothy Lillicrap. A simple neural network module for relational reasoning. *NeurIPS*, 30, 2017.

[23] Yaniv Benny, Niv Pekar, and Lior Wolf. Scale-localized abstract reasoning. In *CVPR*, pages 12557–12565, 2021.

[24] Mikołaj Małkiński and Jacek Mańdziuk. Multi-label contrastive learning for abstract visual reasoning. *arXiv preprint arXiv:2012.01944*, 2020.

[25] Nicolette A Waschl, Ted Nettelbeck, and Nicholas R Burns. The role of visuospatial ability in the raven's progressive matrices. *Journal of Individual Differences*, 2017.

[26] Kaiming He, Xiangyu Zhang, Shaoqing Ren, and Jian Sun. Deep residual learning for image recognition. In *CVPR*, pages 770–778, 2016.

[27] Xander Steenbrugge, Sam Leroux, Tim Verbelen, and Bart Dhoedt. Improving generalization for abstract reasoning tasks using disentangled feature representations. *arXiv preprint arXiv:1811.04784*, 2018.

[28] Steven Spratley, Krista Ehinger, and Tim Miller. A closer look at generalisation in raven. In *ECCV*, pages 601–616, 2020.

[29] Laurens Van der Maaten and Geoffrey Hinton. Visualizing data using t-sne. *Journal of machine learning research*, 9(11), 2008.

Checklist

1. For all authors...
   (a) Do the main claims made in the abstract and introduction accurately reflect the paper's contributions and scope? [Yes]
   (b) Did you describe the limitations of your work? [Yes] Our model has improved the generalization performance by a notable margin on majority of tests in PGM, but further research is needed to reach the human level of generalization.
   (c) Did you discuss any potential negative societal impacts of your work? [N/A]
   (d) Have you read the ethics review guidelines and ensured that your paper conforms to them? [N/A]
2. If you are including theoretical results...
   (a) Did you state the full set of assumptions of all theoretical results? [N/A]
   (b) Did you include complete proofs of all theoretical results? [N/A]
3. If you ran experiments...
   (a) Did you include the code, data, and instructions needed to reproduce the main experimental results (either in the supplemental material or as a URL)? [Yes] We have uploaded the code in the supplemental material.
   (b) Did you specify all the training details (e.g., data splits, hyperparameters, how they were chosen)? [Yes] See section 4.3.
   (c) Did you report error bars (e.g., with respect to the random seed after running experiments multiple times)? [No]
   (d) Did you include the total amount of compute and the type of resources used (e.g., type of GPUs, internal cluster, or cloud provider)? [No]
4. If you are using existing assets (e.g., code, data, models) or curating/releasing new assets...
   (a) If your work uses existing assets, did you cite the creators? [Yes] The datasets used in this work are cited in [5] and [8].
   (b) Did you mention the license of the assets? [N/A]

(c) Did you include any new assets either in the supplemental material or as a URL? [N/A]

(d) Did you discuss whether and how consent was obtained from people whose data you're using/curating? [N/A]

(e) Did you discuss whether the data you are using/curating contains personally identifiable information or offensive content? [N/A]

5. If you used crowdsourcing or conducted research with human subjects...

   (a) Did you include the full text of instructions given to participants and screenshots, if applicable? [N/A]

   (b) Did you describe any potential participant risks, with links to Institutional Review Board (IRB) approvals, if applicable? [N/A]

   (c) Did you include the estimated hourly wage paid to participants and the total amount spent on participant compensation? [N/A]